IS NEAR-SPHERICAL SHAPE "THE NEW BLACK" FOR SMOKE?

Anna Gialitaki [1,2*], Alexandra Tsekeri [1], Vassilis Amiridis [1], Romain Ceolato [3], Lucas Paulien [3] Emmanouil Proestakis [1], Eleni Marinou [1,4], Moritz Haarig [5], Holger Baars [5] and Dimitris Balis [2]

[1] *National Observatory of Athens, IAASARS, Athens, Greece*
[2] *Laboratory of Atmospheric Physics, Physics Department, Aristotle University of Thessaloniki, Greece*
[3] *ONERA, The French Aerospace Lab, Toulouse, France*
[4] *Institute of Atmospheric Physics, German Aerospace Center (DLR), Oberpfaffenhofen, Germany*
[5] *Leibniz Institute for Tropospheric Research (TROPOS), Leipzig, Germany*
**Email: togialitaki@noa.gr*

ABSTRACT

We present smoke lidar measurements from the Canadian fires of 2017. The advected smoke layers over Europe are detected at both tropospheric and stratospheric heights, with the latter presenting non-typical values of the Particle Linear Depolarization Ratio (PLDR) with strong wavelength dependence from the UV to the Near-IR. Specifically, the PLDR values are of the order of 22, 18 and 4% at 355, 532 and 1064 nm respectively. In an attempt to interpret these results, we apply the hypothesis that smoke particles have near-spherical shapes. Scattering calculations with the T-matrix code support other findings in the literature ([1]- [2]), showing that the near-spherical shape (or closely similar shapes as in [2]), is the only shape that has been shown to reproduce the observed PLDR and Lidar Ratio (LR) values of the stratospheric smoke particles at the three measurement wavelengths.

1. INTRODUCTION

Recent studies show that the PLDR of smoke presents large variability ([3] - [7]). Since the PLDR is indicative of particle shape, this variability may be attributed to (a) smoke aerosol mixing with other aerosol types, (b) particles' aging through various atmospheric processes, (c) particle water uptake at different relative humidity conditions. These processes alter the smoke particle shape and composition. Indicatively, the typical PLDR values of aged and fresh tropospheric smoke varies from 2 to 10% at 532 and 355 nm ([3] - [5]), while this value can be larger when smoke is mixed with high depolarizing aerosol types (i.e. dust) ([6] - [7]). Lately, observational evidence of PLDR values that exceed the typical range has been reported. Burton et al. (2015) [8], showed air-borne HSRL measurements of smoke at 8 km altitude, originating from Canadian fires, revealing PLDR values of the order of 20, 9 and 1.8 % at 355, 532 and 1064 nm, respectively. These are also the first reported measurements of smoke PLDR spectral dependence. Other studies validate these high PLDR values for stratospheric smoke particles at 532 nm ([9] - [11]).

In the spotlight of the large-scale Canadian fires of 2017, this unique feature of high values of PLDR with unexpected high spectral dependence for smoke particles raises once again an interesting discussion. Here, we aim to seek for an explanation on the variation of PLDR and LR from UV to Near-IR under the hypothesis that the smoke particles have a near-spherical shape.

Our hypothesis and presented results are a continuation effort on previous work reported in the literature. Specifically, in Mishchenko et al. (2016) [1], the lidar measurements presented in [8] were reproduced considering near-spherical shapes for the smoke particles with an axial ratio 0.9 to 1.2. In Bi et al. 2018 [12], it was showed that the PLDR of near-spherical particles with refractive index of 1.3-1.7 + i0.001- i0.01, can take values up to 100%, depending also on the particle size parameter. However, the results of these studies are limited in terms of reproducing only the PLDR wavelength dependence. Here we make a step further, reproducing also the wavelength dependence of the LR considering near-spherical particles. Our methodology is summarized in Section 2, our results in Section 3 and we conclude in Section 4.

2. METHODOLOGY

2.1 The BERTHA lidar system

The lidar measurements presented in this study were conducted at the Leibniz Institute of Tropospheric Research (TROPOS), with BERTHA multi-wavelength lidar system [13]. The measurements have a 7.5 m vertical resolution, while for the specific case study presented here temporal resolution was 10 sec. The capability of BERTHA to provide independent measurements of the particle extinction coefficient and PLDR at three wavelengths constitutes this lidar system unique within the EARLINET network [14]. The BERTHA measurements used herein are not simultaneous for the particle extinction coefficient and PLDR at 1064 nm, since the 1064 cross-polarized channel had to be exchanged with the 1058 nm rotational Raman channel in order to measure the particle extinction at 1064 nm [15]. The overall duration of this procedure was 20-30 minutes [16]. This shortcoming is not expected to affect the study, since the scene analyzed is very stable in terms of aerosol layering, especially in the stratosphere (Figure 1).

2.2 Scattering calculations

In order to reproduce the unique values and spectral dependence of the PLDR and LR of the stratospheric smoke from the Canadian fires, we used light scattering calculations generated with the T-matrix code [17, 18]. The T-matrix code is based on the exact numerical solution of Maxwell's equations. For the calculations we considered a wide range of refractive indices and effective radii typical for aged smoke, employing near-spherical particles but also soot fractal aggregates.

3. RESULTS

Figure 1 presents the observations from Leipzig, on 22 August 2017, with the 3+3+3 polarization/Raman lidar BERTHA. As it can be seen from the Range Corrected Signal (RCS) at 1064 nm, the stratospheric smoke layer lies between 15 and 16 km, while there is also a smoke layer in the troposphere at 5-6 km. For deriving the smoke optical properties, lidar signals were averaged over a time window of 2.5 hours (20:45 – 23:15 UTC) to achieve satisfying signal to noise ratio (SNR), even at high altitudes. For deriving the PLDR at 1064 nm a time window of 40 min was used (23:50 – 00:30 UTC).

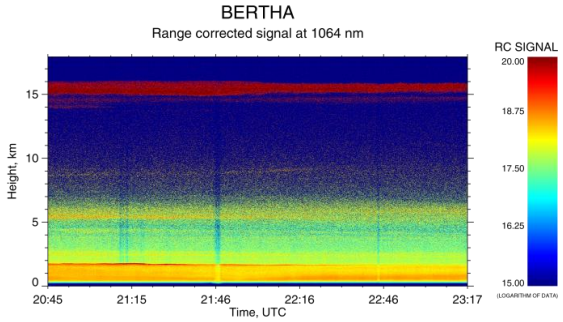

Fig.1. BERTHA RCS at 1064 nm, showing the smoke layers advected from Canada over Leipzig, in the troposphere (5 – 6 km) and in the stratosphere (15 – 16 km).

Figure 2 shows the mean PLDR and LR values of the stratospheric smoke layers and their errors. The LR values are found to be typical for aged smoke particles (40 ± 16) sr at 355 nm, (66 ± 12) sr at 532 nm, which are consistent with what is reported in the literature (i.e. [3] - [7], [19] - [20]), and (92 ± 27) sr at 1064 nm. No significant difference has been detected for the LR values between the tropospheric and stratospheric layers (see [16]), while this does not hold true for the PLDR values. In the case of stratospheric smoke the PLDR values are 22.5, 18.5 and 4% at 355, 532 and 1064 nm, respectively, while in the troposphere they are no higher than 3% at all wavelenghts [16].

Building on the previous studies of [1] and [12] we used near-spherical smoke particles to reproduce the measured PLDR and LR at 355, 532 and 1064 nm in the stratosphere. T-matrix simulations were conducted for a range of refractive index values: m = 1.4 – 1.75 (with step of 0.05) + i(0.005 – 0.045) (with step of 0.005), the particles are considered to follow mono-modal log-normal size distributions with mean effective radii of: r_{eff} = 0.1 to 0.7 μm (with step of 0.05 and a fixed effective variance of v_{eff} = 0.03) and mono-modal normal shape distributions with mean axial ratio: a/b = 0.6 to 1.55 (with step of 0.05 and fixed standard deviation σ_s = 0.05). The fitting of the measurements is performed on the basis of achieving the minimum sum of squares of relative differences between measurements and simulations as shown in Eq. (1), where M_λ^i represents the measured PLDR/LR values at wavelength λ_i, (i = 355, 532, 1064 nm) and S_λ^i the corresponding simulated values. Out of

the results, the solution is accepted based on the requirement that each simulated value has to be within the measurement error (Eq. 2).

$$\sum_{i=1}^{n}\left(\frac{M_\lambda^i - S_\lambda^i}{M_\lambda^i}\right)^2 = min \quad (1)$$

$$S_\lambda^i \leq e(M_\lambda^i) \quad (2)$$

Figure 4 presents the best fit of the measured PLDR and LR at 355, 532 and 1064 nm, calculated for near-spherical smoke particles with mean a/b = 1.4, m = 1.55+ i0.025 and r_{eff} = 0.25 μm (Figure 3). Table 1 summarizes our results for near-spherical particles, in comparison with the Leipzig observations. The T-matrix-calculated PLDR values were found to be 21.8, 18.3 and 4.5 % at 355, 532 and 1064 nm respectively, while the LR values were 41.7, 64.2 and 98.5 sr at 355, 532 and 1064 nm.

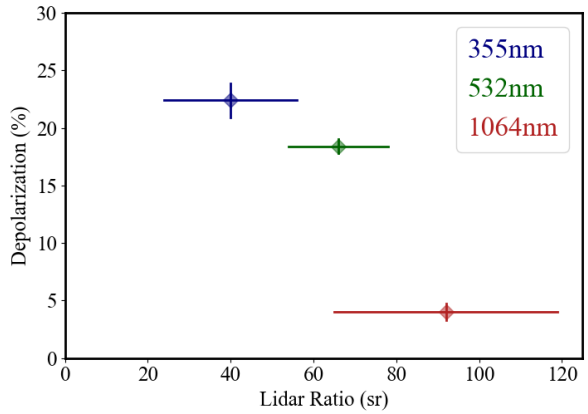

Fig.2 Intensive optical properties of the stratospheric smoke particles at 355, 532 and 1064 nm. All values correspond to the time window 22/8 20:45 – 23:15 UTC, except of the PLDR at 1064 nm which corresponds to the time window 23:50 – 00:30 UTC.

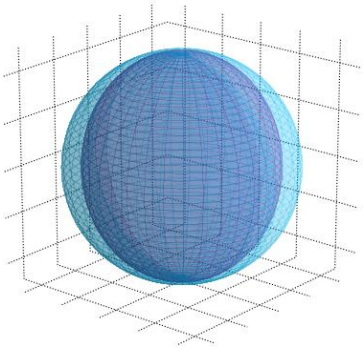

Fig. 3 Near spherical particle (a/b = 1.4, r_{eff} = 0.25 μm) found to reproduce the observed PLDR and LR values at all measurement wavelengths.

A slight deviation from the measured mean values is found at all wavelengths, however all calculated parameters are found to be within the measurement errors.

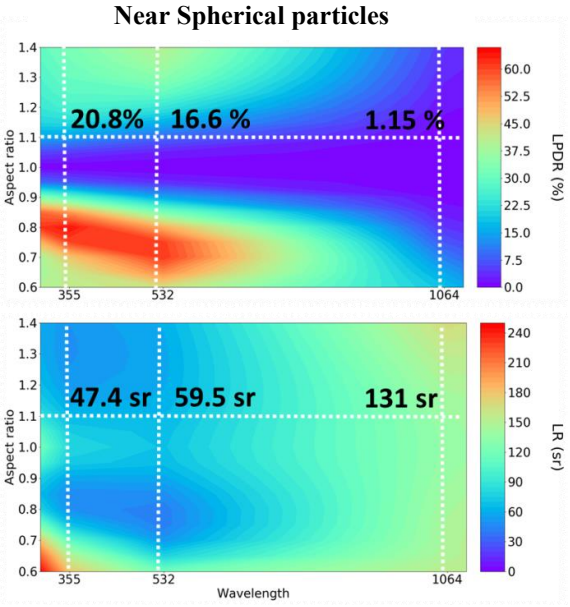

Fig. 4 a) PLDR and **b)** LR, calculated with the T-matrix code for near-spherical smoke particles with r_{eff} = 0.25 μm, v_{eff} = 0.03 and m = 1.55 + i0.025. The measured PLDR and LR at 355, 532 and 1064 nm for near-spherical smoke particles with mean axial ratio a/b = 1.4 (white dash lines).

Table 1. Leipzig measurements vs T-matrix simulations for near spherical particles with mean axial ratio of a/b = 1.4, m = 1.55 + i0.025 and r_{eff} = 0.25μm.

	355	*532*	*1064*
		PLDR	
Obs.	22.4 ± 1.5	18.4 ± 0.6	4.3 ± 0.7
Sim.	21.8	18.3	4.5
		LR	
Obs.	40 ± 16	66 ± 12	92 ± 27
Sim.	41.7	64.2	98.5

In an attempt to examine whether more complicated morphologies can reproduce the observations, we also performed scattering calculations with the Superposition T-Matrix Method (STMM) [21] for highly irregular smoke particles with a simple chain-like fractal morphology (Figure 5). Specifically, we considered a soot fractal aggregate with a fractal

geometry provided by a diffusion-limited cluster-aggregation (DLCA) model [22]. Here, the fractal morphology of the particle is characterized by the fractal pre-factor $k_f = 1.3$, the fractal dimension $D_f = 1.8$, the number of monomers $N = 90$, and the volume-equivalent radius $R_V = 0.55\ \mu m$. The calculated LPDR of the fractal soot aggregate at 355, 532 and 1064 nm are presented in Table 2 for m = 1.42 + i0.02.

Fig. 5 Model morphology of soot fractal aggregate used in STMM simulations.

Although the use of this simple fractal geometry provides significantly large PLDR, it does not reproduce the measured values of both PLDR and LR, as it was also shown in greater detail in [2] (see Fig. 9 and 10). In order to reproduce the measurements for aged smoke particles the fractals need to be coated by other material, producing a shape that closely resembles the near-spherical shape, as shapes for Type-B, size 11, Vr = 20, found in [2], Fig. 4.

Table 2. Leipzig measurements vs superposition T – matrix simulations for a fractal aggregate with m = 1.42 + i0.02, $D_f = 1.8$, $k_f = 1.3$, $R_V = 0.55\ \mu m$.

	355	*532*	*1064*
	PLDR (%)		
Obs.	22.4 ± 1.5	18.4 ± 0.6	4.3 ± 0.7
Sim.	13	10	3

4. CONCLUSIONS

The use of near-spherical shapes explains at a large extent the exceptional PLDR values observed at stratospheric smoke layers over Leipzig, originated by Canadian wildfires. This hypothesis also reproduce the PLDR and LR spectral dependence found, when the aspect ratio is very close to unity for typical refractive index, and size of smoke particles.

ACKNOWLEDGEMENTS

We acknowledge support of this work by the project "PANhellenic infrastructure for Atmospheric Composition and climatE change" PANACEA (MIS 5021516), the Stavros Niarchos Foundation and the European Research Council under the European Community's Horizon 2020 research and innovation framework program / ERC Grant Agreement 725698 (D-TECT).

REFERENCES

[1] M. Mishchenko et al., Applied optics, 55, 9968–9973 (2016)
[2] H. Ishimoto et al., Atmos. Meas. Tech., 12, 107–118 (2019)
[3] D. Müller et al. J. Geophys. Res., 110, D17201, 5 (2005)
[4] D. Nicolae et al. J. Geophys. Res. Atmos., 118, 2956–2965 (2013)
[5] E. Giannakaki et al. Atmos. Chem. Phys., 15, 5429–5442 (2015)
[6] Tesche et al. J. Geophys. Res. 114, D13202 (2009)
[7] I. Veselovskii et al. Atmos. Meas. Tech., 11, 949-969 (2018)
[8] S. P. Burton et al. Atmos. Chem. Phys., 15, 13453 – 3473 (2015)
[9] M. Fromm et al. J. Geophys. Res. Atmos, 113 (2008)
[10] N. Sugimoto et al. SOLA, 6, 93–96 (2010)
[11] F. Dahlkötter et al. Atmos. Chem. Phys., 14, 6111–6137 (2014)
[12] L. Bi et al. Opt. Express, 26 (2018)
[13] M. Haarig et al. Atmos. Chem. Phys., 17, 10767–10794 (2017)
[14] G. Pappalardo et al. Atmos. Meas. Tech., 7, 2389–2409 (2014)
[15] M. Haarig et al. Atmos. Meas. Tech., 9, 4269–4278 (2016)
[16] M. Haarig et al. Atmos. Chem. Phys., 18, 11847-11861 (2018)
[17] P. C. Waterman, Phys. Rev. D, 3, 825 – 839 (1971)
[18] M. Mishchenko et al. J. Quant. Spectrosc. Radiat. Transfer, 60, pp. 309—324 (1998)
[19] T. Murayama et al. Geophys. Res. Lett., 31, L23103 (2004)
[20] M. Fiebig et al. J. Geophys. Res. Atmos., 107 (2002)
[21] D. W. Mackowski, J. Quant. Spectrosc. Radiat. Transfer 133, 264–270 (2014)
[22] S. Jungblut et al. J. Phys. Chem. C, 123 (1), 950–954 (2019)